JOURNAL OF THE KOREAN ASTRONOMICAL SOCIETY
33: 127 ~ 135, 2000

THE EFFECTS OF PLANETARY ROTATION ON THE EXOSPHERIC DENSITY DISTRIBUTIONS OF THE EARTH AND MARS

YONG HA KIM AND SUJEONG SON
Department of Astronomy and Space Science, Chungnam National University, Daejeon, 305-764, Korea
E-mail: ykim@jupiter.chungnam.ac.kr
(Received Sep. 20, 2000; Accepted Oct. 4, 2000)

ABSTRACT

We investigate the effects of planetary rotation on the exospheres of the earth and Mars with simple collisionless models. We develope a numerical code that computes exospheric densities by integrating velocity functions at the exobase with a 10 point Gauss method. It is assumed in the model that atoms above the exobase altitude move collisionlessly on an orbit under the planet's gravity. Temperatures and densities at the exobase over the globe are adopted from MSIS-86 for the earth and from Bougher et al's MTGCM for Mars. For both the earth and Mars, the rotation affects the exospheric density distribution significantly in two ways: (1) the variation of the exospheric density distribution is shifted toward the rotational direction with respect to the variation at the exobase, (2) the exospheric densities in general increase over the non-rotating case. We find that the rotational effects are more significant for lower thermospheric temperatures. Both the enhancement of densities and shift of the exospheric distribution due to rotation have not been considered in previous models of Martian exosphere. Our non-spherical distribution with the rotational effects should contribute to refining the hot oxygen corona models of Mars which so far assume simple geometry. Our model will also help in analyzing exospheric data to be measured by the upcoming Nozomi mission to Mars.

Key words : PLANETS: individual (Earth–Mars) – Planets: atmospheres

I. INTRODUCTION

The exosphere or planetary corona is the vast space above a planetary thermosphere that contains very rare density of neutral gas. Owing to extremely low density collisions between constituents are so infrequent in the exosphere that classical models of this region are based on the assumption of a complete absence of collisions (Öpik and Singer, 1961; Chamberlain 1963). Exospheric densities were calculated in the classical models by assuming a sharp level, called the critical level or the exobase above which constituents move, undisturbed by collisions, along orbital tracks under the planet's gravity. Below the exobase the constituent's velocities were assumed to have an isotropic Maxwellian distribution at a temperature of the thermosphere. The collisionless models for the earth exosphere have since improved by taking into account various effects: non-uniform exobase condition (Vidal-Madjar and Bertaux, 1972), rotational effects (Hartle, 1973), and thermospheric wind effects (Hartle and Mayr, 1976). In order to remove the unnatural assumption of the sharp boundary, Monte Carlo simulation has been applied to the transition region (see review by Fahr and Shizgal, 1983). Later, various collision processes between neutrals and ions in the exosphere were included in Monte Carlo simulations to achieve better accuracy of models (Tinsley et al., 1986; Hodges, 1994). For Mars, collisionless models have been developed for hot oxygen atom corona (Nagy and Cravens, 1988; Ip, 1990; Lammer and Bauer, 1991; Kim et al., 1998). Very recently, Hodges (2000) applied Monte Carlo simulation to the hot oxygen corona of Mars. Since the Martian thermosphere is at low temperature, non-thermal processes, such as dissociative recombination of O_2^+ into hot O atoms, were usually considered as sources for generating high speed to fill the exosphere. However, thermal oxygen atoms are important at low altitudes of the exosphere, which will be shown in this paper. As a base work for building comprehensive models of the Martian exosphere, we here develope collisionless models that include non-uniform conditions at the exobase and planetary rotational effect. We test our computer code by applying to the simple cases for the earth exosphere and then analyze the effects of planetary rotation as well as the relation between conditions at the exobase and exospheric density distributions. Upon confirming the reliability of the code, we use it to calculate density distributions of thermal oxygen atoms in the Martian exosphere, which has not been considered in previous models. The exosphere model for thermal oxygen atoms will be extended by including hot oxygen atoms in future works.

II. MODEL

The exosphere is so dilute that collision between particles be very rare. In the collisionless space, according to Liouville theorem, the momentum distribution function of particles stays constant along the track of particles (cf. Chamberlain and Hunten 1987). The densities at a position in the exosphere, therefore, can

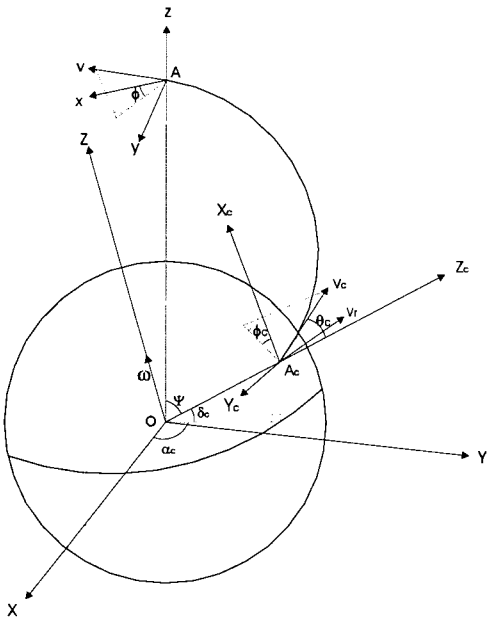

Fig. 1.— Coordinate systems for particles move along a conic orbit from A_c to A. X direction is toward the sun.

be expressed with integration of the momentum distribution function at a position on the exobase, where the particles began orbital motion under the planet's gravity without collision. Figure 1 shows geometry of a particle's orbit between a position A in the exosphere and A_c at the exobase. From the momentum and energy conservation laws, velocities and flight angles of particles can be related as

$$V_c^2 - 1 = V^2 - y \quad (1)$$

$$\frac{V \sin\theta}{y} = V_c \sin\theta_c, \quad (2)$$

where

$$y = \frac{r_c}{r}, \quad V = \frac{v}{v_{esc}}, \quad Vc = \frac{v_c}{v_{esc}} \quad (3)$$

The subscript c indicates the exobase, and the angle θ, the flight angle, is measured from the local vertical axis. The equation of all the conic orbit has a general form as

$$r = \frac{p}{(1 + e\cos\nu)} \quad (4)$$

and the semi-letus rectum, p and eccentricity, e can be expressed as functions of y, V, θ,

$$p(y, V, \theta) = \frac{2r_c V^2 \sin^2\theta}{y^2} \quad (5)$$

$$e(y, V, \theta) = \sqrt{1 - 4V^2 \sin^2\theta(y - V^2)/y^2}. \quad (6)$$

The angle from A_c to A on the orbital plane, Ψ can be computed from difference in true anomalies, ν - ν_c. The longitude, α_c and latitude, δ_c of A_c are determined with spherical geometric relations from α and δ of A, the orbit angle Ψ, and an azimuthal angle of the orbit, ϕ with respect to the poleward direction. The longitudes, α and α_c, are measured from the sun direction, since both the thermosphere and exosphere vary with local time. At the exobase, we assume that the particles are under thermal equilibrium at a local temperature $T_c(\alpha_c, \delta_c)$ and thus follow a Maxwellian distribution. The phase distribution function at the exobase can be expressed as

$$f_c = N_c(\alpha_c, \delta_c)\left(\frac{2\pi k T_c(\alpha_c, \delta_c)}{m v_{esc}^2}\right)^{-\frac{3}{2}} \times exp\left(-\frac{mMGV_c^2}{r_c k T_c(\alpha_c, \delta_c)}\right), \quad (7)$$

where N_c is the local density at the exobase, m, M, G and k are particle and planet's mass, gravitational and Boltzmann constants, respectively. When the particle leaves the exobase, the velocity of planetary rotation should be added to its local velocity, v_c. Thus the v_c should be replaced with $v_c + v_{rot}$, and after some algebra the above expression is modify to

$$f_c = N_c(\alpha_c, \delta_c)\left(\frac{2\pi k T_c(\alpha_c, \delta_c)}{m v_{esc}^2}\right)^{-\frac{3}{2}} \times exp\left[-\frac{mMG}{r_c k T_c(\alpha_c, \delta_c)}(V_c^2 + \omega^2 r_c^2 \cos^2\delta_c^2 - 2\omega r_c \cos\delta_c V_c \sin\theta_c \sin\phi_c)\right], \quad (8)$$

where ω is the angular velocity of planetary rotation. Since vectors perpendicular to the orbital plane from

A and A_c should have the same angle with respect to the planet's rotation pole, the relation

$$\sin\phi\cos\delta = \sin\phi_c\cos\delta_c \quad (9)$$

is satisfied. Using this relation and equation (1) and (2), the distribution function become

$$\begin{aligned} f_c &= N_c(\alpha_c,\delta_c)\left(\frac{2\pi kT_c(\alpha_c,\delta_c)}{mv_{esc}^2}\right)^{-\frac{3}{2}} \\ &\times exp[-\frac{mMG}{r_c kT_c(\alpha_c,\delta_c)}(V^2+1-y \\ &+ \omega^2 r_c^2\cos^2\delta_c^2 - \frac{2\omega r_c\cos\delta V\sin\theta\sin\phi}{y})]. \quad (10) \end{aligned}$$

The Liouville theorem allows to compute the density, $N(\alpha,\delta)$, at a position A in the exosphere from the distribution function, f_c, as

$$N(\alpha,\delta) = \int_{pop} f_c(\alpha_c(\alpha,\delta),\delta_c(\alpha,\delta))d^3V. \quad (11)$$

The ranges of integration are selected by considering orbital characteristics of particles. For ballistic orbits, the velocity V at the point, A, should be less than $\sqrt{y}$ for the particle not to escape from the planet. The ballistic orbits can be divided into two cases, one for which all flight angles are possible, and the other for which the flight angle is limited for the orbit to intersect with the exobase. The former case requires the velocity V less than $y/\sqrt{(1+y)}$ since the flight angle, $\theta = 90°$ (then $\theta_c = 90°$) should be possible when the points, A and A_c are the apogee and perigee of the orbit. For the latter case, $y/\sqrt{(1+y)} < V < \sqrt{y}$, the flight angle requires to be in the range $\theta < \theta_m$, for an ascending orbit, and $\pi - \theta_m < \theta < \pi$ for a descending orbit. The condition, $\theta = \theta_m$ or $\pi - \theta_m$, occurs when the particle leaves the exobase horizontally, that is $\theta_c = 90°$. Applying this condition to equations (1) and (2), the maximum angle, θ_m, can be computed from the expression,

$$\sin\theta_m = \frac{y}{V}\sqrt{V^2+1-y}. \quad (12)$$

The range of θ between θ_m and $\pi - \theta_m$ consists of satellite orbits outside the exobase. The satellite orbits are excluded in our model since they can not relate the thermosphere to the exosphere in our collisionless model. However, rare number of collisions between particles or with solar photons may detract particles from thermosphere to satellite orbits, and thus add densities in the exosphere. On the other hand, hyperbolic orbits surely contribute to the density at the point A, if they originate below the exobase. The velocity, V, should be greater than $\sqrt{y}$ and the flight angle, θ, should be less than θ_m for the ascending hyperbolic orbit. The descending hyperbolic orbit cannot connect the thermosphere to the exosphere. The integration for computing densities at a point A in the exosphere, therefore, may be written as

$$\begin{aligned} N(\alpha,\delta) &= \int_0^{V_b}\int_0^{\pi}\int_0^{2\pi} f_c V^2\sin\theta dV d\theta d\phi \\ &+ \int_{V_b}^{\sqrt{y}}\int_0^{\theta_m}\int_0^{2\pi} f_c V^2\sin\theta dV d\theta d\phi \\ &+ \int_{V_b}^{\sqrt{y}}\int_{\pi-\theta_m}^{\pi}\int_0^{2\pi} f_c V^2\sin\theta dV d\theta d\phi \\ &+ \int_{\sqrt{y}}^{\infty}\int_0^{\theta_m}\int_0^{2\pi} f_c V^2\sin\theta dV d\theta d\phi. \quad (13) \end{aligned}$$

We develope a code to compute the above tripple integration with the Gauss 10-point method. In our model we assume that atoms leaving the thermosphere have velocities of a Maxwellian distribution with a temperature at the exobase altitude. The exobase altitudes for hydrogen atom on the earth and oxygen atom on Mars are assumed to be 500 km and 190 km, respectively. We adopt the standard empirical thermosphere model of MSIS-86 for earth case (Hedin, 1987), and a theoretical thermosphere model of MTGCM for Mars (Bougher et al, 1999).

III. RESULTS AND DISCUSSION

(a) A Simple Model

We first consider a simple model for the earth's hydrogen exosphere to test our code. The densities and temperatures of the exobase were assumed to vary in sine function as shown in Fig. 2. In order to characterize the effects of temperature and density variations, we intentionally placed the maxima of the temperature and density at noon and midnight, respectively. The actual thermospheric conditions, of course, vary complexively with local times, seasons, geomagnetic activities, solar activities, and other unknown factors. With the assumed conditions of the exobase, we compute hydrogen densities of the exosphere on the equatorial plane, and show the relative densities along the local time in Fig. 3. The solid, dotted, and dashed lines indicate the cases for zero, one and two times the speed of earth's rotation included, respectively. We include the model with two times the rotation because the thermosphere may have global circulation that can add up to the planetary rotation speed when atoms leave the exobase. The density distributions in Fig. 3 near the midnight show a maximum at 1.1 earth radius (ER), but plunge into a minimum at high altitudes. This is because the low altitude exosphere can be reached by nearly all hydrogen atoms from the exobase and thus is affected directly by the density variation at the exobase. However, the high altitude exosphere can only be reached by high velocity atoms, and thus reflects more sensitively the temperature variation at the exobase. Due to nature of the exponential function in a Maxwellian distribution, small increase in temperature

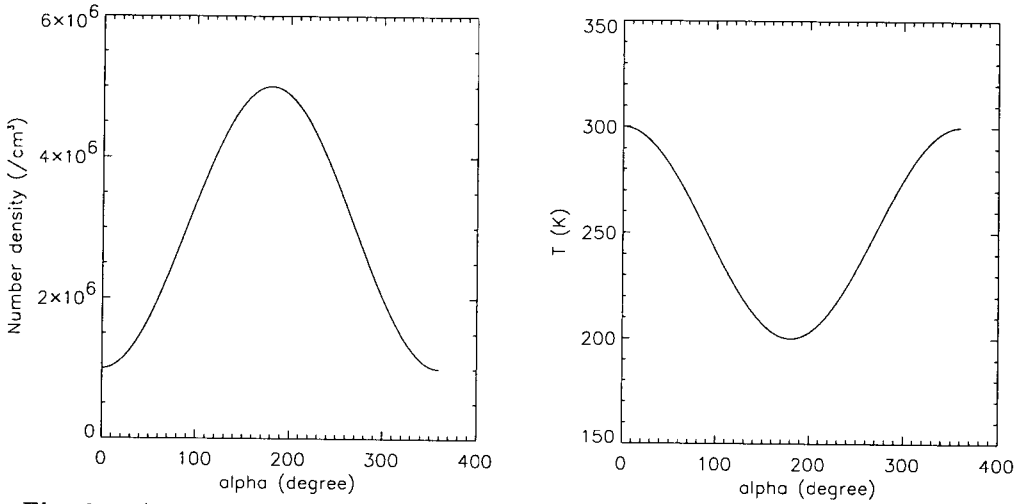

Fig. 2.— Assumed density and temperature variations at the exobase on the equatorial plane.

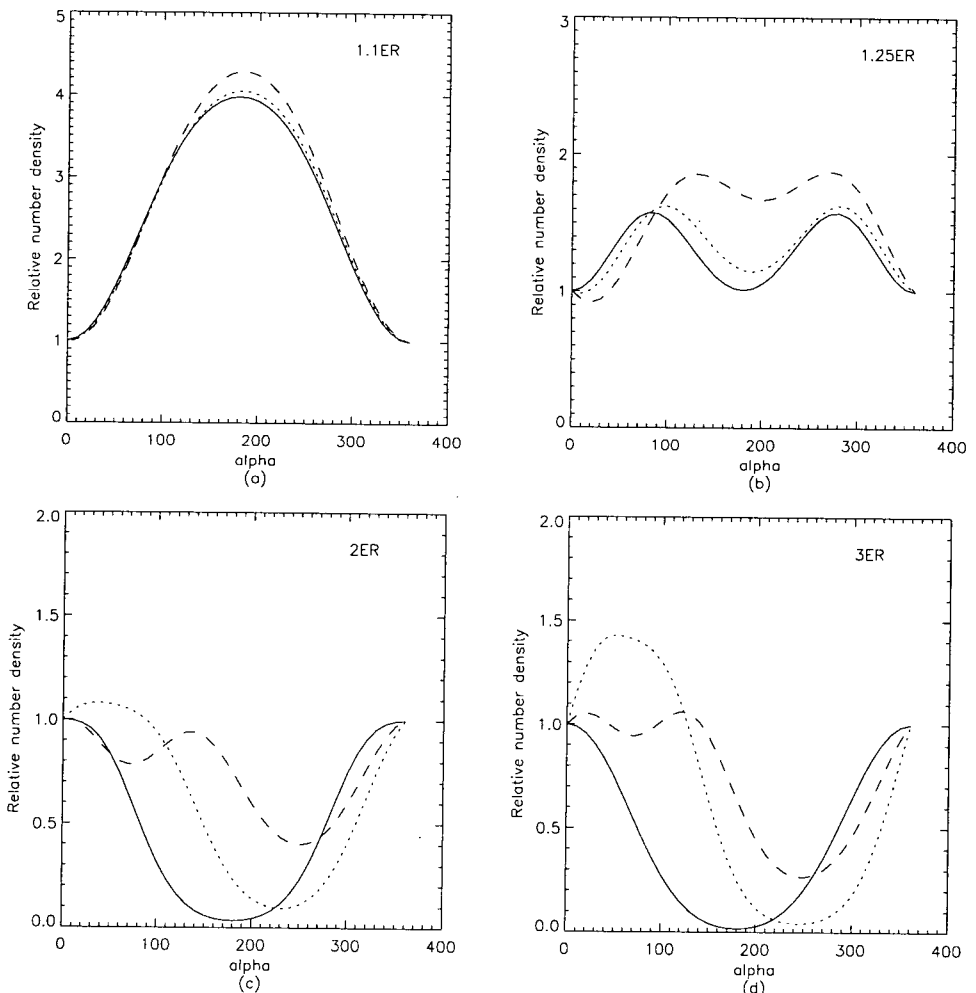

Fig.3.— Relative density distribution at different altitudes for three rotational speeds (solid line: no rotation, dotted line: 1× rotation, dashed line: 2× rotation).

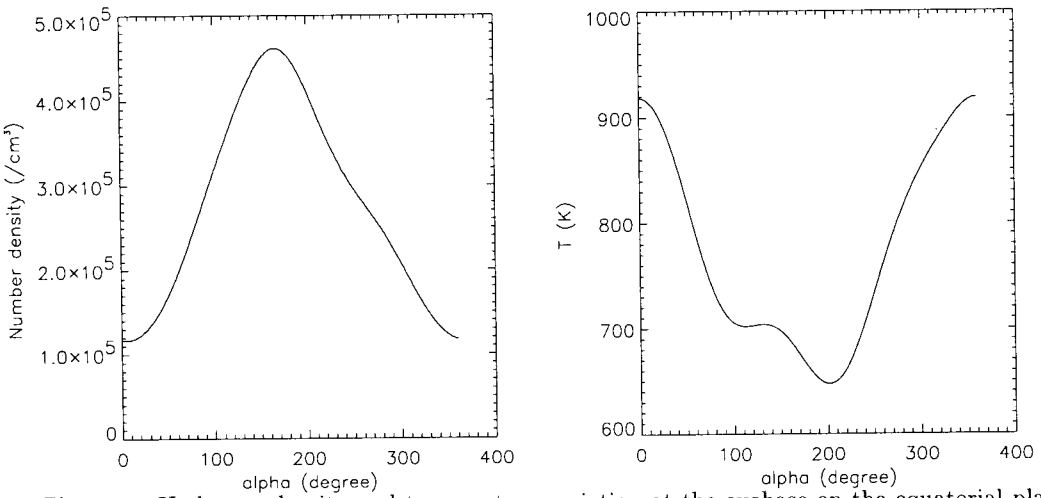

Fig. 4.— Hydrogen density and temperature variation at the exobase on the equatorial plane from MSIS-86 model (day of vernal equinox, $F_{10.7} = 50$, $A_p = 0$).

causes large increase in portion with high velocity that can reach the high altitudes. The amplitude of density variation in Fig. 3 decreases with altitude because densities at high altitudes are contributed from the wide range of exobase, resulting in the averaging effect of the exobase conditions. Fig. 3 also show clearly that the planetary rotation cause the distribution significantly shifted toward the rotational direction.

(b) A Model for the Earth's Hydrogen Exosphere

The earth's exosphere consists mainly of hydrogen atoms originated from the thermosphere below. Since a hydrogen atom is very light, its thermal speed is fast enough to travel through the vast space of the exosphere. For example, the thermal speed of a hydrogen atom at 810 K (about the average temperature of the exobase) can make it reach to 1.25 ER, and twice the speed can up to 6 ER. We calculate the hydrogen densities in the exosphere with the exobase conditions that were adopted from the empirical standard thermosphere model, MSIS-86. The MSIS-86 model provides temperatures and densities at the exobase for all latitude and local time. For $F_{10.7} = 50$ and $A_p = 0$ on the day of vernal equinox, Fig. 4 shows the density and temperature variations at the exobase on the equatorial plane. The variation patterns of both temperature and density are very similar to our simple model considered in the previous section. However, the exobase conditions in other latitudes, which is different from those for the equatorial plane, are also included in the model calculation. Fig. 5 shows relative density distributions of hydrogen atoms in the exosphere. As in the simple model, the distributions at low and high altitudes resemble the variations of density and temperature, respectively, at the exobase on the equator. The transition occurs around 3 ER, where the distribution appears more or less uniform because the number of atoms originated from the minimum temperature region ($\alpha \sim 180°$) is about equal to that of atoms from the maximum density region. Above the transition altitude only high speed hydrogen atoms can reach so that temperature at the exobase is more important factor to influence the exospheric densities. Planetary rotation affects the distributions significantly, especially at high altitudes, as shown with dotted and dashed lines in Fig. 5. At altitude of 2 ER the distributions with rotation clearly shift eastward (larger α) due to the addition of rotational speed to thermal speed when atoms leave the exobase. However, at higher altitudes the distributions with rotation show non-uniform shifts from those without rotation, which were not seen in the simple model. This is because the densities at high altitudes are affected by exobase conditions in wide ranges of latitude and longitude. For example, atoms at 15 ER originate from the exobase area with $\sim 40°$ radius. Atoms at high latitudes leave the exobase with different rotational speeds from those at the equator, which makes the distribution change rather complexively. Hydrogen atoms in the exosphere have been observed as Ly-α corona from space (Thomas and Bohlin, 1972). Solar Ly-α photons are resonantly scattered by the exospheric hydrogen atoms, resulting in bright geocorona around the earth. The observed distribution of hydrogen atoms has a maximum in the antisolar direction, known as the "geotail". The "geotail" phenomena is mainly owing to solar wind interaction with exospheric hydrogen atoms, which was not considered in our collisionless model. Our simple collisionless model should thus be used only for analysis of observations of the lower exosphere, such as ground based observations of Balmer-alpha emission, which we plan to carry out with an all-sky camera in near future.

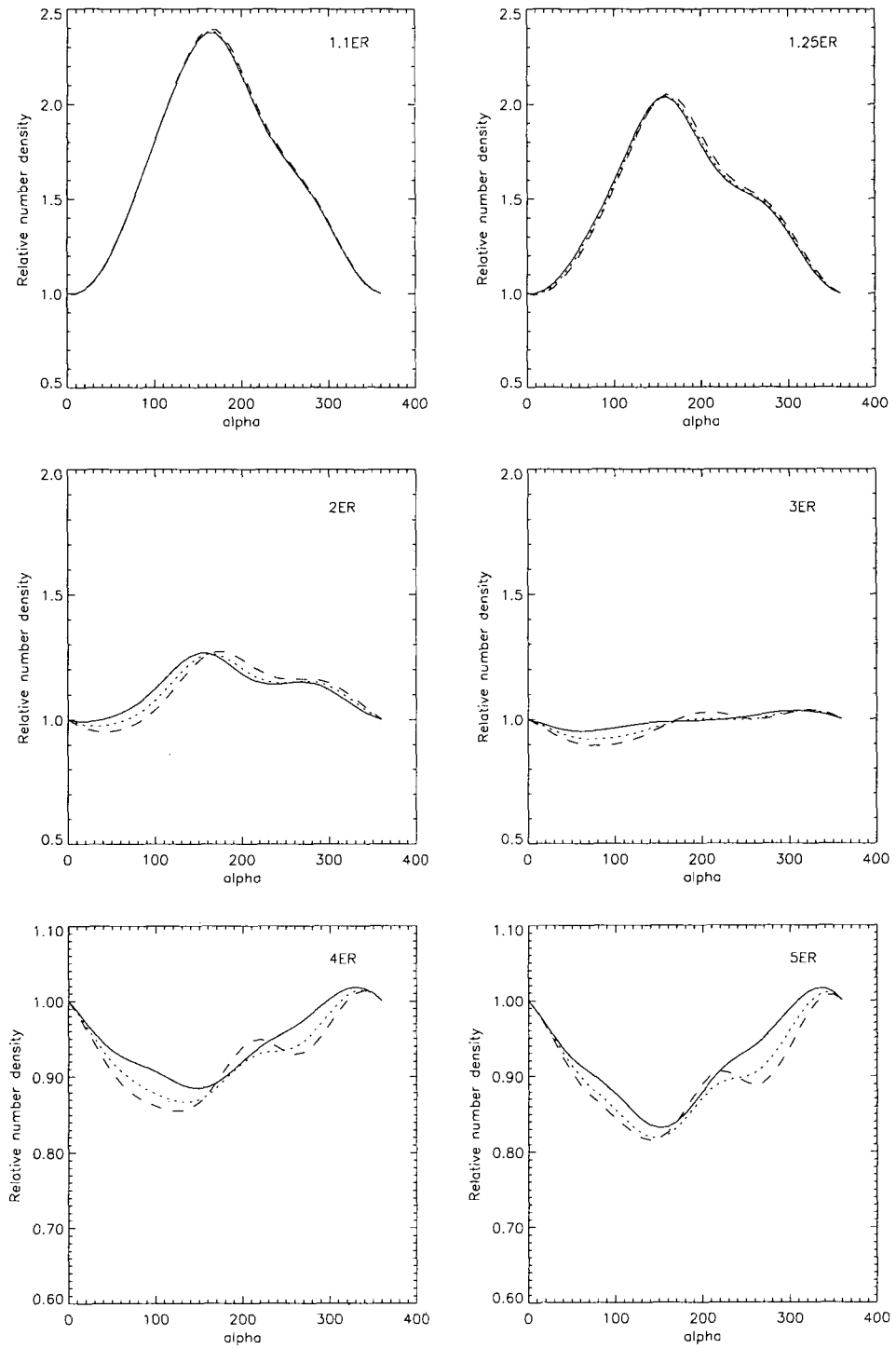

Fig. 5.— Relative density distributions of hydrogen atoms on the equatorial plane of the earth (solid line: no rotation, dotted line: 1× rotation, dashed line: 2× rotation).

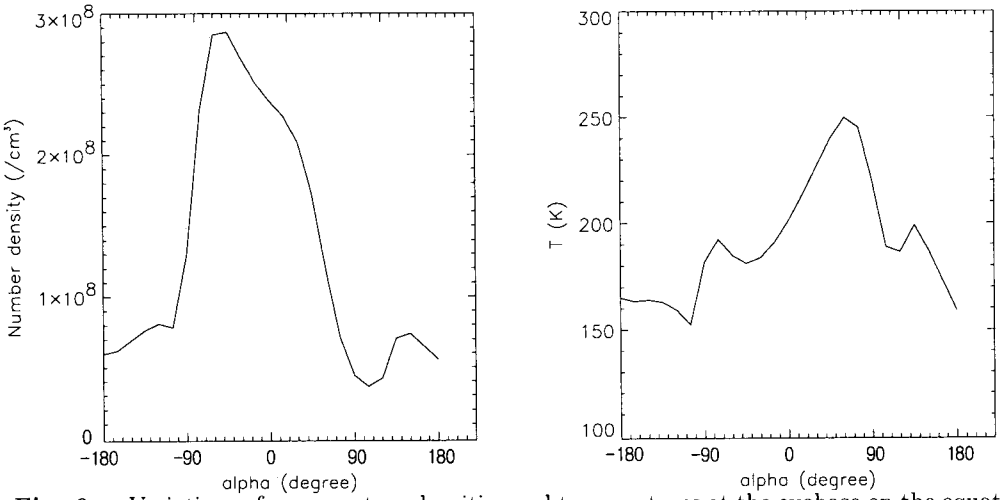

Fig. 6.— Variations of oxygen atom densities and temperatures at the exobase on the equatorial plane of Mars from MTGCM.

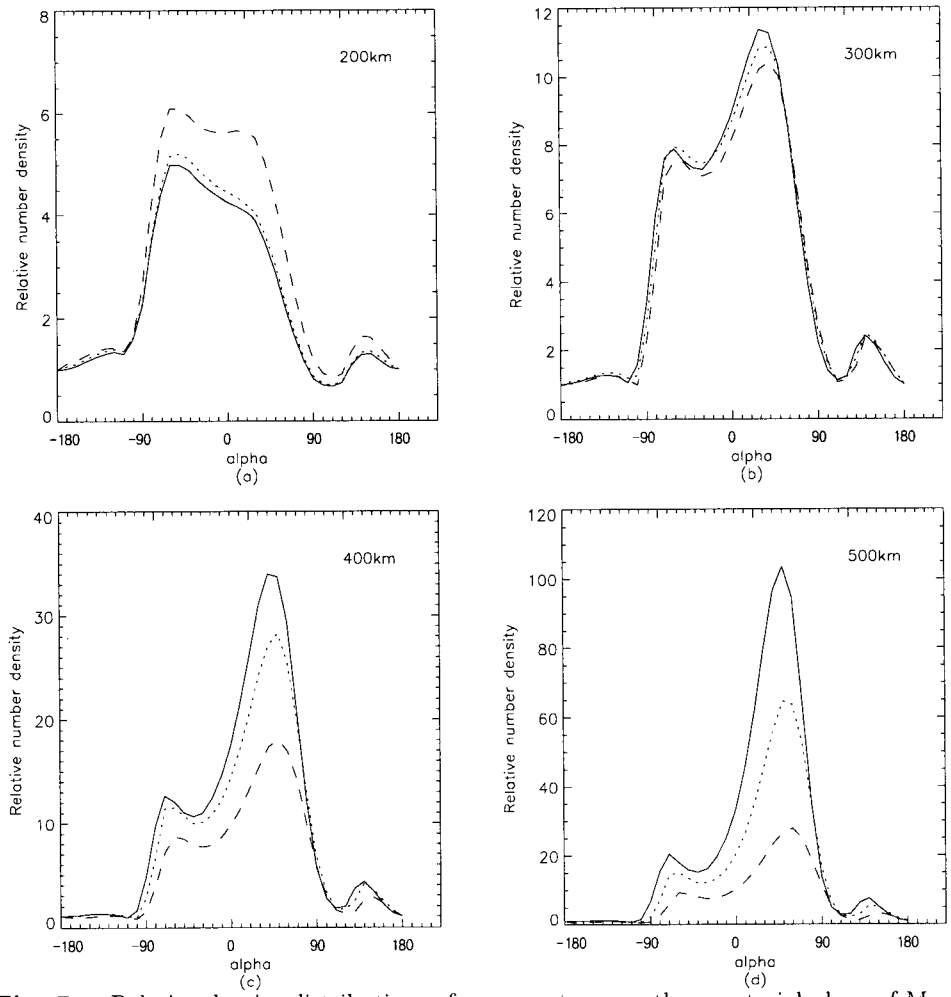

Fig. 7.— Relative density distributions of oxygen atoms on the equatorial plane of Mars (solid line: no rotation, dotted line: 1× rotation, dashed line: 2× rotation).

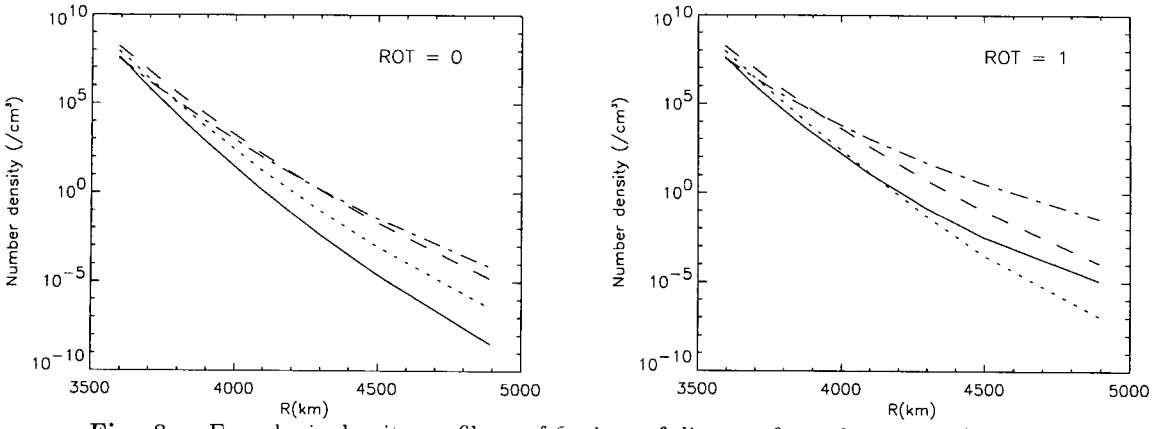

Fig. 8.— Exospheric density profiles as functions of distance from the center of Mars for four direction on the equatorial plane. Left and right figures are for models without and with rotation, respectively (solid line : $\alpha = -180°$, dotted line : $\alpha = -90°$, dashed line : $\alpha = 0°$, dashed and dotted line : $\alpha = 90°$).

(c) A Model for the Martian Oxygen Exosphere

The Martian exosphere is thought to consist mainly of hot oxygen atoms originated from non-thermal processes in the thermosphere. Despite the low gravity of Mars, thermal oxygen atoms do not reach high altitudes in the exosphere due to low temperature of the Martian thermosphere. A thermal speed of oxygen atoms at 2000 K can make them reach altitudes less than 700 km, which is only 500 km above the exobase. The model we develope here is only for thermal oxygen atoms at lower part of the Martian exosphere. The model for hot oxygen atoms will be presented in the future since it involves with different methodology on production and transportation of hot oxygen atoms. As in the earth case, we adopt a standard thermospheric model of Mars (MTGCM) from Bougher et al (1999) to define the exobase conditions. The temperatures and oxygen atom densities are presented in Fig. 6 on the equatorial plane at the exobase altitude of 190 km. Since temperatures and densities on other latitudes are not available from the MTGCM, we assume that the conditions are the same as on the equator. Although recent aero-braking experiments of Mars Global Surveyor provided valuable information on the Martian thermosphere (Keating et al, 1998), measurement data are still scarce, compared to that of earth or even Venus, to construct reliable global models of the thermosphere. With uncertain constraints on the exobase conditions, our intention is only to estimate the effect of planetary rotation on oxygen atom distribution in the lower part of the exosphere. Fig. 7 shows relative density distributions of oxygen atoms at four altitudes on the equatorial plane. The solid lines are for the non-rotating case, and dotted and dashed lines indicate models with rotation speed of one and two times Mars's rotation, respectively. As in the earth models, the distributions resemble the density variation of Fig. 6 at very low altitudes and then quickly become reminiscent to the temperature variation as the altitude increases. The amplitude of the distributions also increases with the altitude. This is because only small tail portion of the thermal velocity distribution, which varies sensitively with temperature, can make atoms reach to high altitudes. The planet's rotational speed causes the distributions to shift toward the rotating direction, as shown in Fig. 7. The addition of the rotational speed also mitigates the sensitive dependence of the distributions on temperatures. This effect can be seen in Fig 7, where the relative distributions with the rotational speeds have smaller amplitude than those without the rotational speed. The addition of the rotational speed boosts atoms to higher altitudes than the thermal speed alone allows. Consequently, the models with rotational speeds have larger densities at all altitudes than the non-rotating model, as shown in Fig. 8. The effect is especially important for the Martian exosphere since its thermospheric temperature is low. The rotating model shows increase in densities at an altitude of 1000 km 5 - 10 times those of the non-rotating model, depending on the longitude. Previous models for the Martian exosphere ignored this rotation effect by just assuming barotropic density distribution of thermal oxygen atoms above the exobase (J. Kim et al., 1998; Hodge, 2000). Although the previous models were concerned only with hot oxygen corona of Mars that dominates the exosphere above $\sim$ 1000 km, the hot oxygen corona models should be revised for the oxygen densities below 1000 km that are affected by factors of 5 - 10 due to the planet's rotation.

IV. CONCLUSION

In order to investigate the effects of planetary rotation on the exosphere, we have developed a numerical code that computes exospheric densities by integrating velocity functions at the exobase, with assumption

that above the exobase particles move collisionlessly on an orbit under the planet's gravity. The model shows that exospheric density distribution around the equator at low and high altitudes resemble density and temperature variations at the exobase, respectively. This can be understood by noting that high altitudes can be reached only with high speeds whose populations change sensitively with temperature. For both the earth and Mars, the planet's rotation affects the exospheric density distribution significantly in two ways: (1) the variation of the exospheric density distribution is shifted toward the rotational direction with respect to the variation at the exobase, (2) the exospheric densities in general increase over the non-rotating case. The rotational effects are more significant for lower thermospheric temperatures and more evident in distributions at high altitudes. Both the enhancement of densities and shift of the exospheric distribution due to rotation have not been considered in previous models of the Martian exosphere. Our non-spherical distribution with the rotational effects should contribute to refining the hot oxygen corona models of Mars, and thus lead to better understanding of the solar wind interactions with the Martian exosphere. Our model will also help in analyzing exospheric data to be measured by the upcoming Nozomi mission to Mars.

The authors wish to acknowledge the financial support of the Korea Science and Engineering Foundation (96-0702-03-01-3).

REFERENCES

Bougher, S. W., Engel, S., Roble, R. G., & Foster, B. 1999, J. Geophys. Res., 104, 16,591

Chamberlain, J. W. 1963, Planet. Space Sci., 11, 901

Chamberlain, J. W., & Hunten, D. M. 1987, Theory of Planetary Atmospheres

Fahr, H. J., & Shizgal B. 1983, Rev. Geophys. Space Phys., 21, 75

Hartle, R. E. 1973, Planet. Space Sci., 21, 2123

Hartle, R. E., & Mayr, H. G. 1976, J. Geophys. Res., 81, 1207

Hedin, A. E., 1987, J. Geophys. Res., 92, 4649

Hodges, R. R. 1994, J. Geophys. Res., 99, 23,229

Hodges, R. R. 2000, J. Geophys. Res., 105, 6971

Ip, W. H. 1990, Geophys. Res. Lett., 17, 2289

Keating, G. M., et al., 1998, Science, 279, 1672

Kim, J., Nagy, A. F., Fox, J. L., & Cravens, T. E.1998, J. Geophys. Res. 103, 29,339

Lammer, H., & Bauer, S. J. 1991, J. Geophys. Res., 96, 1819

Nagy, A. F., & Cravens, J. E. 1988, Geophys. Res. Lett., 15, 433

Öpik, E. J., & Singer, S. F. 1961, Phys. Fluids, 4, 221

Thomas, G. E., & Bohlin, R. C. 1972, J. Geophys. Res., 77, 2752

Tinsley, b. A., Hodges, R. R., & Rohrbaugh, R. P. 1986, J. Geophys. Res., 91, 1363

Vidal-Madjar, A., & Bertaux, J. L. 1972, Planet. Space Sci., 20, 1147